

# Microstructural characterization and gas sensing properties of solution precursor plasma-sprayed zinc oxide (ZnO) nanostructured coatings

C. Zhang, Yangzhou/CN, H. Li, Ningbo/CN, P. He, M. Planche, H. Liao, Belfort/F, M. Olivier, M. Debliquy, Mons/B

ZnO nanostructured coatings have been prepared on Al<sub>2</sub>O<sub>3</sub> substrates fitted with interdigitated Au electrodes on one side and a Pt heater on the other side, and explored as a gas sensor. ZnO coatings were deposited by solution precursor plasma spray (SPPS) using zinc acetate Zn(CH<sub>3</sub>COO)<sub>2</sub> aqueous solution as spraying precursor solution. The SPPS process has proven its simplicity and reliability in realizing polycrystalline ZnO coatings as verified by XRD structural analysis. The FE-SEM images confirmed that the coatings are nanostructured with grain size ranging from 50 to 100 nm. The surface morphology and grain size of coatings is influenced by H<sub>2</sub> gas flow rate in plasma forming gas. The sensing properties of sensors based on the SPPS ZnO coatings to NO<sub>2</sub> were characterized and the sensors showed good sensitivity to NO<sub>2</sub> gas in sub-ppm range.

## 1 Introduction

In the last decades, increasing attention has been paid on resistive type gas sensors based on semiconducting metal oxides [1–3], because they can be widely applied for the monitoring of explosive, flammable and toxic gases in industrial communities. The sensing mechanism of semiconducting gas sensors is based on the change in the electrical resistances of the sensitive layer in the presence of target gas molecules. The gas response is known to be influenced by the coating microstructure, crystal structure, chemical state, sensor design, etc. [4–6] Nanostructured and porous sensitive coatings are favorable for obtaining high performance sensors from the viewpoints of gas diffusion permeation and active sites [2].

ZnO is a basic material for semiconducting gas sensor [7]. Different fabrication processes, e.g., CVD[8], sputtering[9], vacuum evaporation [10], were used for the preparation of sensitive layers. However, many researchers found that the complexity and high cost of these traditional techniques for coating deposition. The use of another deposition method, deposition from solution precursor plasma spray (SPPS) [11], was proposed for overcoming the above mentioned technological problems. In SPPS, a liquid chemical precursor droplet is injected into the plasma jet. All physical and chemical reactions, such as evaporation, pyrolysis, crystallization and coating formation, occur in one single step. However, the coating is also built up by overlapping and stacking of deposited splats. The production of coatings directly from solution makes SPPS technique not only a straightforward process but also attractive for developing nanostructures with an easy control [12].

In the present paper, ZnO coatings have been fabricated by SPPS process on Al<sub>2</sub>O<sub>3</sub> substrates kept at room temperature. The structural, morphological and electrical parameters of SPPS coatings have been investigated and correlated. Sensors based on the obtained coatings have been subjected to gas sensing tests. The sensors showed a high response to nitrogen dioxide (NO<sub>2</sub>) when operated at different temperatures.

## 2 Experimental methods

### 2.1 Coating preparation

ZnO coatings were deposited using the F4MB plasma torch (Sulzer Metco, Switzerland), which was attached to a six-axis ABB robotic arm, as shown in Fig. 1. The primary plasma gas was argon with a flow rate of 12 L·min<sup>-1</sup>, and the secondary plasma gas was hydrogen with a flow rate of 5 or 8 L·min<sup>-1</sup>. The arc current was 600 A and consequently the plasma power was 31.2 or 34.4 kW respectively. The feedstock used was a saturated aqueous solution of zinc acetate Zn(CH<sub>3</sub>COO)<sub>2</sub>. The thickness of ZnO coating was controlled at 2.5 μm. The spraying parameters were listed in Table 1.

Table 1: Solution precursor plasma spraying parameters.

Parameters	Value
arc current	600 A
spraying distance	100 mm
argon flow rate	30 L·min <sup>-1</sup>
hydrogen flow rate	5 or 8 L·min <sup>-1</sup>
argon powder carrier gas	0.5 × 10 <sup>5</sup> Pa
nozzle diameter	0.24 mm
flow rate of solution	13.5 mL·min <sup>-1</sup>
anode internal diameter at torch exit	6 mm

### 2.2 Coating characterization

The phase composition of the obtained coating was determined using X-ray diffraction with a Cu K $\alpha$  radiation (XRD, D5000, Siemens, Germany). The XRD patterns were collected in a 2 $\theta$  range from 20° to 75° with a scanning rate of 1° min<sup>-1</sup>, and from 30 to 39°C with a rate of 0.05° min<sup>-1</sup>. A field-emission scanning electron microscope (FE-SEM, SU8020, Hitachi, Japan) was used to characterize the coating morphology.

### 2.3 Gas sensing tests

Sensing characteristics of the sensors based on the ZnO coatings were measured in a Teflon chamber. The sensors were connected to a home-designed system to measure electrical resistances. After the electrical resistances of the sensors were stable in reference air and waiting for another 30 min, 10 ppm NO<sub>2</sub>

(commercial gas, Praxair NV, Belgium) was introduced in the reference air with controlled flow rates to get the desired concentrations of the target gases. The concentrations of the target gases were calculated by doing a division of the flow rates of the commercial gas and total gas (commercial gas + reference gas). In this work, 0.12-1 ppm NO<sub>2</sub> was used as target gas.

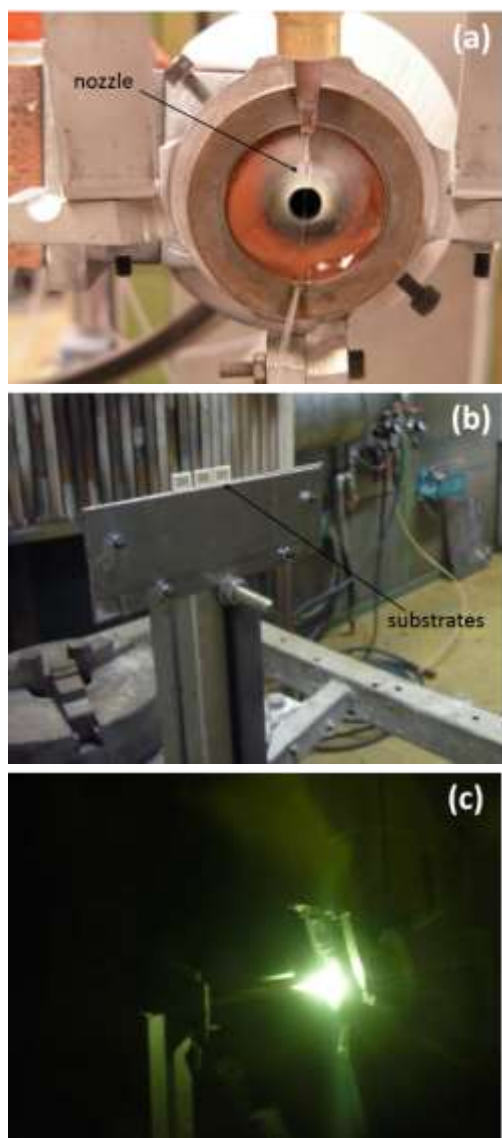


**Fig.1:** Experimental setup of solution precursor plasma spraying for ZnO coating: (a) liquid nozzle; (b) sensor substrate and (c) plasma plume during deposition.

The gas sensors were tested at temperatures ranging from 250 to 325 °C. Sensor response was defined as  $S = R_{\text{gas}}/R_{\text{air}}$  in which  $R_{\text{gas}}$  and  $R_{\text{air}}$  were the resistances of coatings in the presence of target gas and reference gas, respectively. The relative humidity (R.H.) of the reference gas was measured at 25°C before being introduced in the test chamber by mixing dry air and wet air (after bubbling in deionized water). In this study, the moisture level of reference air was controlled at R.H. 50%, unless specially mentioned.

## 2.2 Results and discussion

**Fig. 2** shows XRD patterns of the ZnO coatings. XRD patterns also show Au and Al<sub>2</sub>O<sub>3</sub> peaks which were emitted from the Al<sub>2</sub>O<sub>3</sub> substrates and gold electrodes below the coating. These results confirm that the as-sprayed coatings deposited with 5 L•min<sup>-1</sup> or 8 L•min<sup>-1</sup> H<sub>2</sub> have polycrystalline nature and hexagonal wurtzite crystal structure (PDF: 36-1451). Further to observe on **Fig. 2b**, it can be found that the peak of 5 L•min<sup>-1</sup> H<sub>2</sub> coating (abbreviated as 5L coating in this paper) was slightly broader compared with 8 L•min<sup>-1</sup> H<sub>2</sub> coating (abbreviated as 8L coating). The crystallite size of the two SPPS coatings were calculated using Debye Scherrer Formula,  $d = K\lambda/\beta\cos\theta$ , where  $\lambda$  is the wavelength of the X-ray radiation (Cu K $\alpha$  = 0.15406 nm),  $K$  is a constant taken as 0.89,  $\beta$  is full width at half maximum height and  $\theta$  is the diffraction angle. To estimate average crystallite sizes, the three most intense peaks, i.e., (110), (002) and (101) at 31.77, 34.42 and 36.25°, were used.

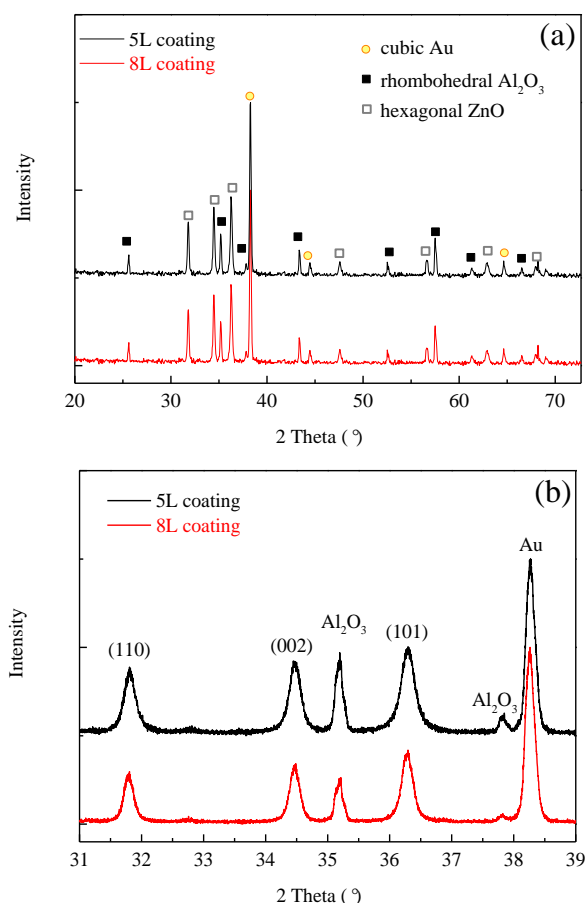


**Fig. 2:** XRD patterns of the SPPS ZnO coatings: (a) rapid scan and (b) slow scan.

The average crystallite sizes for the two coatings are 31.8 nm and 39.4 nm respectively. As well known, the hydrogen flow rate in the plasma gas has an important influence on the plasma enthalpy and plasma thermal conductivity. The increase in hydrogen flow rate enhances the evaporation, precipitation, and pyrolysis of the solution droplet, and induced larger crystallite size in the deposited coating.

**Fig 3** and **4** present the surface morphology of the two ZnO coatings. It can be found that the temperature of plasma plume ( $H_2$  flow rate) plays an important role in the coating microstructure. The 5L coatings as shown exhibit a smooth surface whereas the 8L coatings give a rough surface. The agglomeration in 5L coating was less and smaller compared to that in 8L coating. The droplets of the zinc acetate solution undergo accelerated chemical reactions in the high temperature plasma flame to form semi-molten/molten particles before impacting on the substrate. The following reaction can be used to describe the pyrolysis in the plasma jet.

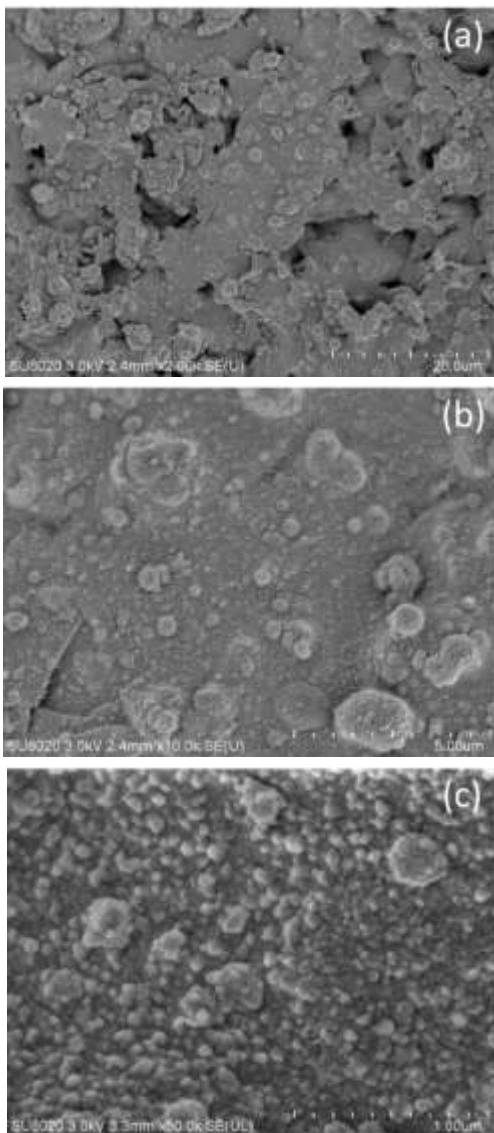
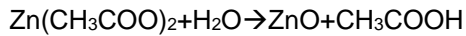


**Fig. 3:** Surface morphology and ZnO coating prepared by 5L  $H_2$  plasma: (a) 2000x; (b) 10 000x; and (c) 50 000x.

In 5L coating, it seems that ZnO particles were deposited one by one. On the contrary, ZnO particles existing in the form of agglomerates were presented in 8L coatings, which make the coating have a rougher

surface. The formation of agglomerates may be attributed to higher temperature of the plasma plume when more  $H_2$  is used. The particles those formed during precipitation and pyrolysis of the solution droplets could possibly fuse together into agglomerates before exiting the plume. Further to observe **Fig. 4c** and **5c**, it can be found that the particles in 5L coatings retained the angular shape while the particles in 8L  $H_2$  coatings were well melted, which can also be ascribed to the difference in the temperature of the plasma plume.

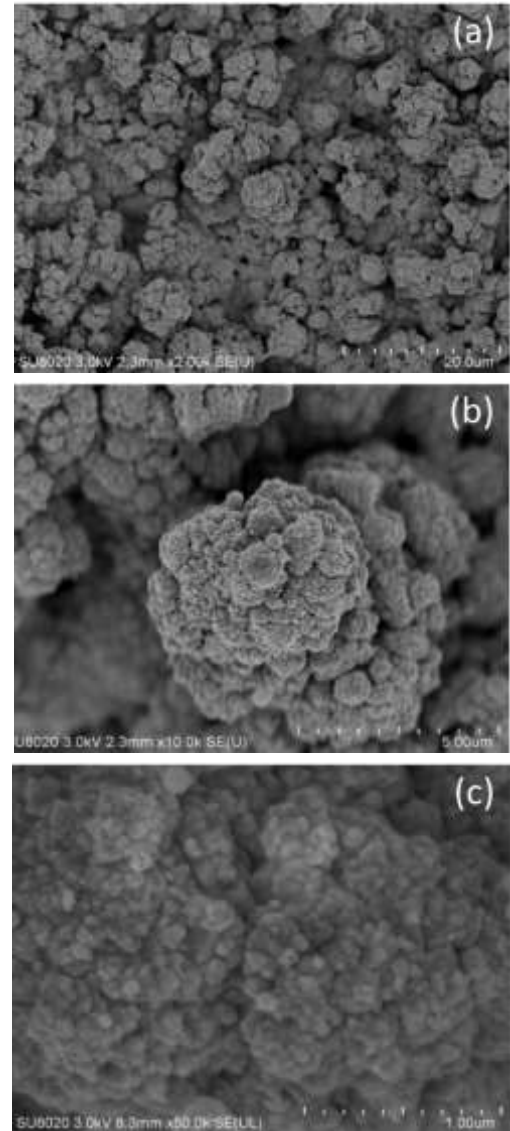


**Fig. 4:** Surface morphology and ZnO coating prepared by 8L  $H_2$  plasma: (a) 2000x; (b) 10 000x; and (c) 50 000 x.

It can be found from **Fig. 5** that the base resistance of 8L coating was higher than the 5L  $H_2$  coating. The base resistances of the two coatings were about 5.2 and 24 K $\Omega$  at 250°C, respectively. This should be ascribed to the different microstructure of the two coatings. The 8L  $H_2$  coating has a rough and porous structure whereas the 5L coating is smooth and dense. Moreover, it can be observed that the base resistances decreased with

the increase in working temperature from 250 to 325°C, which is a typical behavior of semiconductor.

The electrical resistances of sensors are plotted against time with NO<sub>2</sub> concentration steps ranging from 0.12 to 1 ppm in air with R.H. 50%, as shown in **Fig. 5**. The NO<sub>2</sub> concentration at each step is displayed by blue dash line in the figure. The positive response in electrical resistance agrees with the previous results [13].

As well known, ZnO is an n-type semiconductor and NO<sub>2</sub> is an oxidizing gas. When NO<sub>2</sub> molecules reach on the surface of ZnO coating, the resistance of ZnO increases due to the increase in thickness of electron depleted layer. It was reported that the electron affinity of NO<sub>2</sub> (2.27 eV) is higher than that of O<sub>2</sub> (0.44 eV)[14], which results in thickening of electron depleted layer and an increase in electrical resistance. The two sensors exhibited different responses to NO<sub>2</sub>, especially at lower temperature. At 250°C, the response of 5L coating to 1 ppm NO<sub>2</sub> at 250°C was about 1.05 and that of the 8L coating was as high as 2.6 even when the NO<sub>2</sub> concentration was as low as 0.12 ppm, indicating that the gas sensors developed in this study have high a detectability and the gas sensors with 8L H<sub>2</sub> coating show a better detectability. When the working temperature increases, the sensor response becomes rapid but low, particularly for the 8L coating. When the temperature reaches 325°C, the two sensors present almost the same responses to NO<sub>2</sub>. At low temperature, the porous microstructure is favorable for gas diffusion, which might be the reason of high response for 8L coating. At high temperature, due to the high diffusion rate, the diffusion was not anymore a bottleneck and the two sensors present almost same responses. However, the adsorption of the gas is unfavorable at high temperature.

Metal oxide sensors are often sensitive to humidity [15]. The presence of water species influences the discrimination ability of a metal oxide-based gas sensor. Therefore, for potential applications, the humidity as main interfering agent, should be considered. It was previously reported that R.H. significantly influenced the sensor signal [13]. The effect of humidity on the sensors based on the SPPS ZnO coatings was studied under the dynamic operation mode. As displayed in **Fig. 6**, the sensors were subjected to sensing test with 0.25 ppm NO<sub>2</sub> at 300°C with R.H. ranging from 0 to 100%.

The sensing characteristics showed that the R.H. had significant influence on the response when R.H. changed from 0 to 10%. The response to 0.25 ppm NO<sub>2</sub> was decreased from 1.7 to 1.6 while the base resistance changed from 15.5 K to 12.6 K when R.H. increased from 0 to 10%. When the R.H. was further increased above 10%, there was no obvious change in base resistance and sensor response. Therefore, it can be concluded that water vapor does not hinder NO<sub>2</sub> detection, especially when R.H. lies above 10%.

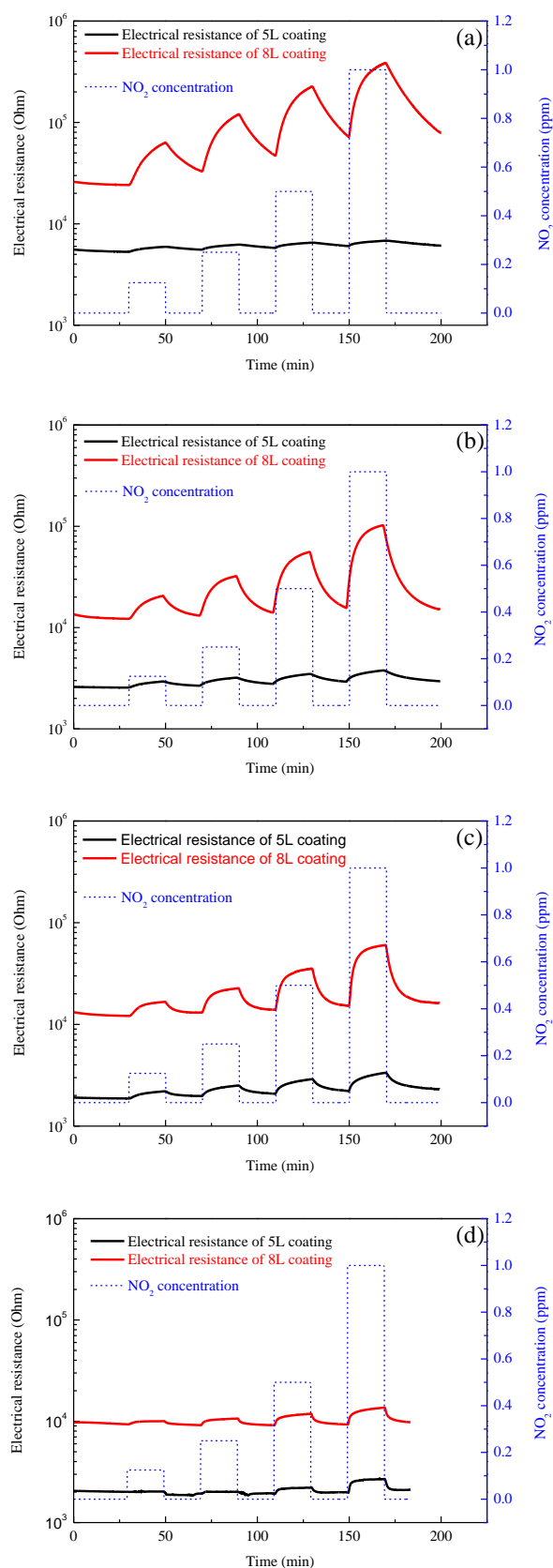


**Fig. 5:** Electrical resistance of the ZnO sensors in function of 0.12-1 ppm NO<sub>2</sub> at (a) 250°C; (b) 275°C; (c) 300°C and (d) 325°C.

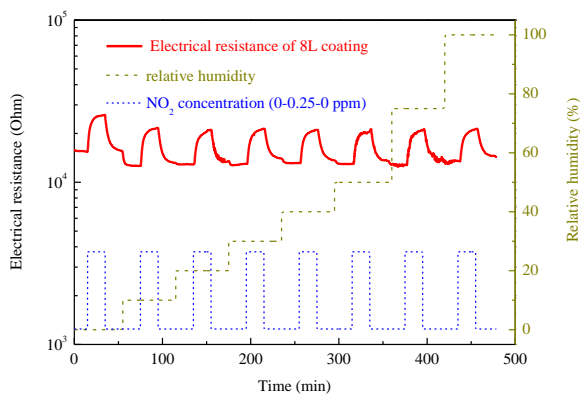


**Fig. 6:** Effect of gas humidity on the electrical resistance response of the sensor to 0.25 ppm NO<sub>2</sub>.

#### 4 Conclusions

In this work, ZnO sensitive coatings were fabricated by solution precursor plasma spraying (SPPS) technique. The sensors based on the obtained ZnO sensitive coatings demonstrated a high sensitivity to NO<sub>2</sub>. The deposition of ZnO sensitive layers using SPPS technique from Zn(CH<sub>3</sub>COO)<sub>2</sub> aqueous solution is straightforward. The as-sprayed coatings present nanostructured and well-crystallized hexagonal ZnO. The H<sub>2</sub> flow rate in plasma forming gas has a strong influence on the microstructure and consequently the sensing properties of the coatings. The obtained ZnO coating prepared by 5 L·min<sup>-1</sup> H<sub>2</sub> in plasma jet presented smooth surface whereas the one deposited by 8 L·min<sup>-1</sup> H<sub>2</sub> in plasma jet showed rough and porous structure. The sensors based on the ZnO coatings show high responses towards NO<sub>2</sub> in the concentration range of 0.12–1 ppm at a working temperature range of 250–325°C. The ZnO sensors prepared by 8 L·min<sup>-1</sup> H<sub>2</sub> plasma presented high response than that by 5 L·min<sup>-1</sup> H<sub>2</sub> plasma, especially at low temperature. However, when the temperature was increased at 325°C, there was no significant difference between two sensors. The humidity has a slight effect on the base resistance and response of the sensor when R.H. is increased from 0 to 10%. When R.H. is further increased above 10%, it had no significant effect on the sensing characteristics of the sensor.

#### 3 Literature

- [1] Simon, I., Bârsan, N., Bauer, M. and Weimar, U.: Micromachined metal oxide gas sensors: opportunities to improve sensor performance. *Sensors and Actuators B: Chemical* 73 (2001), pp. 1–26.
- [2] Afzal, A., Cioffi, N., Sabbatini, L. and Torsi, L.: NO<sub>x</sub> sensors based on semiconducting metal oxide nanostructures: Progress and perspectives, *Sensors and Actuators B: Chemical* 171–172 (2012), pp. 25–42.
- [3] Wetchakun, K., Samerjai, T., Tamaekong, N., Liwhiran, C., Siriwong, C., Kruefu, V. et al.: Semiconducting metal oxides as sensors for

environmentally hazardous gases, *Sensors and Actuators B: Chemical* 160 (2011), pp. 580–591.

- [4] Korotcenkov, G.: The role of morphology and crystallographic structure of metal oxides in response of conductometric-type gas sensors. *Materials Science and Engineering: R: Reports* 61 (2008), pp. 1–39.
- [5] Yamazoe, N.: Toward innovations of gas sensor technology. *Sensors and Actuators B: Chemical* 108 (2005), pp. 2–14.
- [6] Vallejos, S., Khatko, V., Calderer, J., Gracia, I., Cane, C., Llobet, E. et al.: Micro-machined WO<sub>3</sub>-based sensors selective to oxidizing gases. *Sensors and Actuators B: Chemical* 132 (2008), pp. 209–215.
- [7] Azad, A., Akbar, S., Mhaisalkar, S., Birkefeld, L. and Goto K.: Solid-state gas sensors: A Review, *Journal of The Electrochemical Society* 139 (1992), pp. 3690–3704.
- [8] Barreca, D., Bekermann, D., Comini, E., Devi, A., Fischer, R., Gasparotto, A. et al.: 1D ZnO nano-assemblies by Plasma-CVD as chemical sensors for flammable and toxic gases, *Sensors and Actuators B: Chemical* 149 (2010), pp. 1–7.
- [9] Peng, X., Sajjad, M., Yang, B. and Feng, P.: Studies of structural evolution and sensing properties of ZnO nanocrystalline films, *Applied Surface Science* 257 (2011), pp. 4795–4800.
- [10] Abdulgafour, H., Hassan, Z., Yam, F. and Chin, C.: Sensing devices based on ZnO hexagonal tube-like nanostructures grown on p-GaN heterojunction by wet thermal evaporation. *Thin Solid Films* 540 (2013), pp. 212–220.
- [11] Karthikeyan, J., Berndt, C., Tikkanen, J., Reddy, S. and Herman, H.: Plasma spray synthesis of nanomaterial powders and deposits. *Materials Science and Engineering: A* 238 (1997), pp. 275–286.
- [12] Fauchais, P., Etchart-Salas, R., Rat, V., Coudert, J., Caron, N. and Wittmann-Ténéze, K.: Parameters controlling liquid plasma spraying: solutions, sols, or suspensions. *Journal of Thermal Spray Technology* 17 (2008), pp. 31–59.
- [13] Zhang, C., Debliquy, M. and Liao, H.: Deposition and microstructure characterization of atmospheric plasma-sprayed ZnO coatings for NO<sub>2</sub> detection, *Applied Surface Science* 256 (2010) 5905–5910.
- [14] Hyung, J., Yun J., Cho, K., Hwang, I., Lee, J. and Kim, S.: Necked ZnO nanoparticle-based NO<sub>2</sub> sensors with high and fast response, *Sensors and Actuators: B. Chemical* 140 (2009) 412–417.
- [15] Vlachos, D., Skafidas, P. and Avaritsiotis, J.: The effect of humidity on tin-oxide thick-film gas sensors in the presence of reducing and combustible gases. *Sensors and Actuators B: Chemical* 25 (1995), pp. 491–494.